

## Infrared Photometry of Solar Active Regions

M. Sobotka<sup>1,2</sup>, M. Vazquez<sup>1</sup>, M. Sanchez Cuberes<sup>1</sup>, J. A. Bonet<sup>1</sup> & A. Hanslmeier<sup>3</sup>

<sup>1</sup>*Institute de Astrofísica de Canarias, E-38200 La Laguna, Tenerife, Spain.*

<sup>2</sup>*Astronomical Institute, Academy of Sciences of the Czech Republic, CZ-25165 Ondřejov, The Czech Republic.*

<sup>3</sup>*Institut für Geophysik, Astrophysik und Meteorologie, Universitätsplatz 5, A-8010 Graz, Austria.*

**Abstract.** Simultaneous time series of broad-band images of two active regions close to the disk center were acquired at the maximum ( $0.80\ \mu\text{m}$ ) and minimum ( $1.55\ \mu\text{m}$ ) continuum opacities. Dark faculae are detected in images obtained as weighted intensity differences between both wavelength bands. The elements of quiet regions can be clearly distinguished from those of faculae and pores in scatter plots of brightness temperatures. There is a smooth transition between faculae and pores in the scatter plots. These facts are interpreted in terms of the balance between the inhibition of convective energy transport and the lateral radiative heating.

*Key words.* Solar photosphere—faculae—pores.

### 1. Introduction

Observations of active photospheric structures in the infrared are of particular interest, because the opacity minimum is at  $1.6\ \mu\text{m}$ , so that the deepest layers of the photosphere can be probed at this wavelength. Foukal and his colleagues have published a series of papers based on such observations (see Foukal *et al.* 1990) and reported that many faculae are dark at the disk center. Moran, Foukal & Rabin (1992) found that the dark infrared contrast increases with the magnetic flux beyond a threshold value of about  $2 \times 10^{18}\ \text{Mx}$ . Similar observations with spatial resolution of  $1''$  were obtained by Wang *et al.* (1998). In this work we use the infrared photometry of faculae and pores to obtain information about their brightness temperatures in the layers corresponding to the minimum and maximum continuum opacities.

### 2. Observations and data analysis

Series of broad-band CCD images of active regions were obtained at the Swedish Vacuum Solar Telescope (Observatorio del Roque de los Muchachos, La Palma) simultaneously in two channels:  $\lambda = 0.8000 \pm 0.0025\ \mu\text{m}$  (continuum opacity maximum) and  $\lambda = 1.5542 \pm 0.0046\ \mu\text{m}$  (continuum opacity minimum). We observed two active

regions close to the center of solar disk:

- (1) 23rd June 1997, 08:09-09:24 UT, NOAA 8055, a growing group of very small pores.
- (2) 25th June 1997, 08:31-10:07 UT, NOAA 8056, a rapidly developing group of large pores.

After the bias and gain corrections, all frames were normalized to the mean intensity of the undisturbed photosphere  $I_{\text{phot}}$ . The images show details near the diffraction limit of the telescope ( $0.''45$  for  $0.80 \mu\text{m}$  and  $0.''89$  for  $1.55 \mu\text{m}$ ). The frames were aligned, de-stretched, and corrected for the theoretical point-spread function of the telescope. Acoustic waves were removed by subsonic filtering. Frames in both channels were re-sampled to a common scale  $0.''166 \text{ pixel}^{-1}$ . To enable a direct comparison of intensities in both wavelength bands the  $0.80 \mu\text{m}$  images were degraded to the resolution of the  $1.55 \mu\text{m}$  ones.

Using the models of a plage (Solanki & Steenbock 1988), quiet photosphere (Gingerich *et al.* 1971), and a small Sunspot (Collados *et al.* 1994) as proxies of real structures, we found that the differences between the effective formation heights of the  $0.80 \mu\text{m}$  and  $1.55 \mu\text{m}$  continua increases with decreasing mean temperature of the model: 28 km for the plage, 41 km for the quiet photosphere, and 64 km for the small spot.

### 3. Results

To compare the intensities in both wavelength bands we computed weighted difference images  $I_{\text{dif}} = F \cdot [I(1.55) - 1] - [I(0.80) - 1]$ , where "1" stands for normalized  $\bar{I}_{\text{phot}}$  and the factor  $F = [\Delta I_{\text{rms}}^{\text{QR}}(0.80)] / [\Delta I_{\text{rms}}^{\text{QR}}(1.55)]$ , calculated from the rms granular contrasts in the quiet region (QR) for each pair of frames, enhances the contrast at  $1.55 \mu\text{m}$ . This enhancement is necessary because  $\Delta I_{\text{rms}}$  in the  $1.55 \mu\text{m}$  band is lower than that in  $0.80 \mu\text{m}$  by factor of about 2.3 and a simple subtraction of images does not give a clear result. The difference images (Fig. 1) show dark structures which look

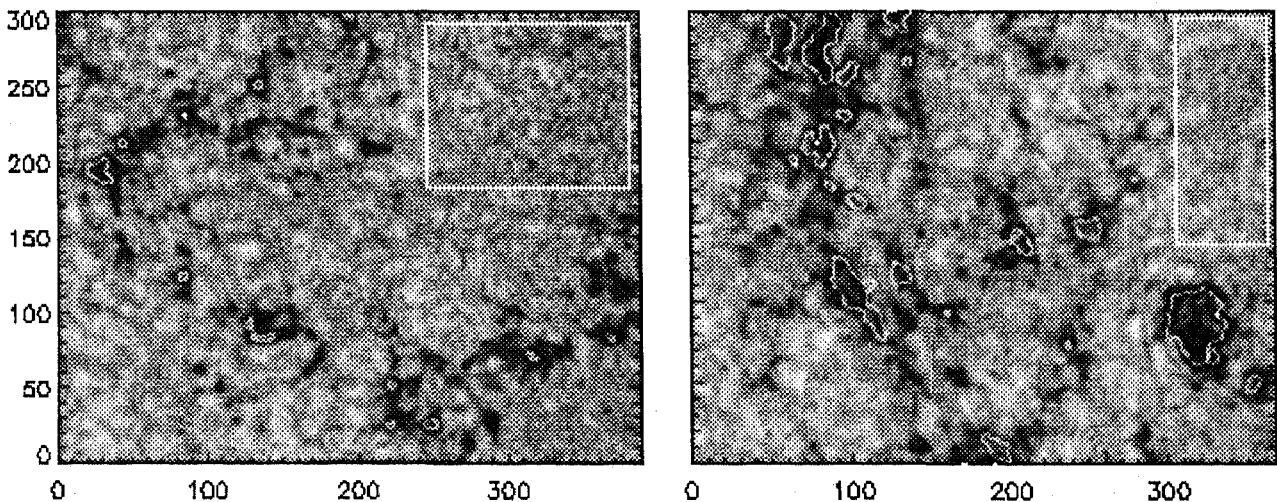


**Figure 1.** Difference images of NOAA 8055 (left) and NOAA 8056 (right) showing dark faculae and pores. The contours indicate borders of pores for  $\lambda 0.80 \mu\text{m}$ . White rectangles enclose quiet regions. The coordinate unit is 1 pixel, i.e.,  $0.166''$ .

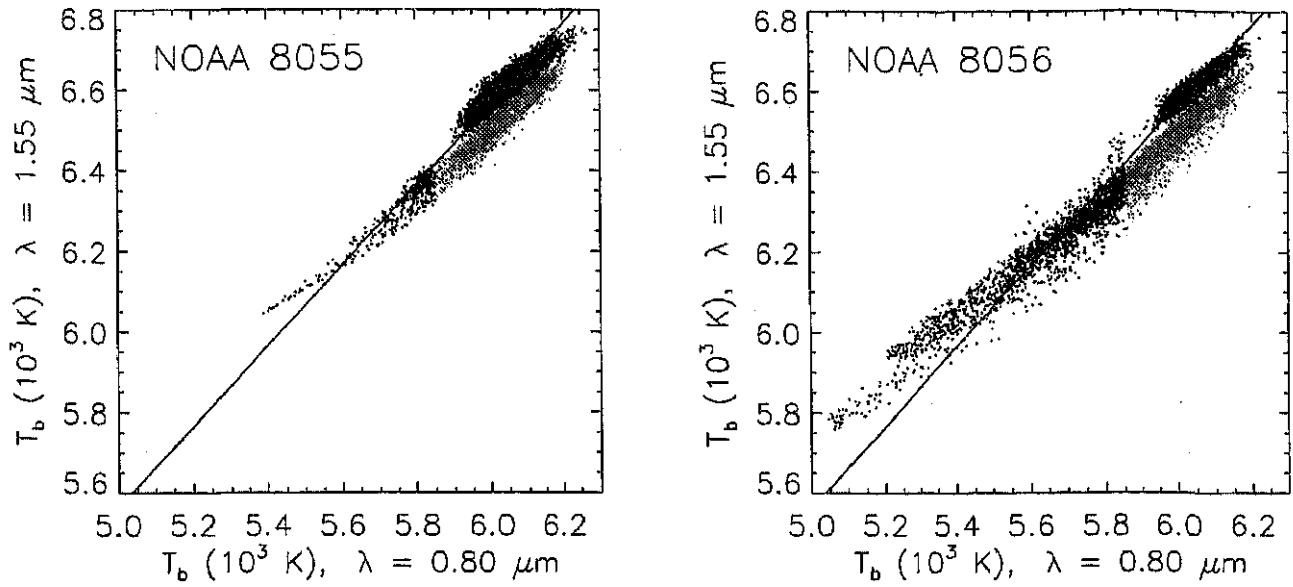


**Figure 2.** Scatter plots of brightness temperatures. Elements of quiet regions and of pores are black, facular elements are gray.

very similar to plages or faculae. The comparison of histograms of intensity distributions in QRs and in dark structures has shown that these darkenings appear due to reduced intensities in the  $1.55 \mu\text{m}$  band as compared to  $0.80 \mu\text{m}$ , so that they correspond to dark faculae.

The normalized intensities were converted to the absolute ones using the calibration factors of Neckel & Labs (1984) and Makarova, Roshchina, & Sarychev (1994), and the brightness temperatures  $T_b$  were computed for each position in the best frames of the series. Pixel-to-pixel scatter plots of  $T_b(1.55)$  versus  $T_b(0.80)$  are shown, in Fig. 2. The pixels belonging to QRs are clearly distinguished from those of faculae and the pixels of pores smoothly extend the cloud of facular pixels toward lower temperatures. The temperature difference  $r T_b = T_b(1.55) - T_b(0.80)$  is an important parameter which depends on the temperature stratification in the atmosphere. The straight line in the scatter plots represents the constant temperature difference  $r T_b(\text{QR}) = 560 \text{ K}$ , corresponding to an average QR. It can be seen that in magnetized regions  $\Delta T_b$  gradually increases with decreasing temperature. All facular pixels show  $r T_b$  lower than the quiet ones. Some parts of the pores have  $r T_b < r T_b(\text{QR})$ , similar to faculae. These parts are observed in  $r T_b$  maps as "rings" outlining the borders of pores. Inner parts of pores are characterized by  $r T_b > \Delta T_b(\text{QR})$ .

#### 4. Discussion

Magnetic field is distributed in the photosphere in the form of discrete elements of different sizes and filling factor. When the magnetic flux reaches a certain value, a facula is formed and the inhibition of convective energy transport reduces the temperature in the lowest photospheric layers, observed at  $1.55 \mu\text{m}$ . In the upper layers, this temperature deficit is balanced by lateral radiative heating, so that faculae are nearly as hot as their surroundings. This explains the discontinuity between QRs and faculae in the temperature scatter plots. In case of pores, the size of magnetic features is so large that the lateral radiative heating cannot compensate the temperature deficit due to the inhibition of convective energy transport, and photospheric

layers become cooler than the surroundings at all heights. The observed increase of  $r T_b$  with decreasing  $T_b$  could be partially explained by increasing difference between the effective formation heights of the 0.80 and 1.55  $\mu\text{m}$  continua, indicated by model calculations (see Sect. 2), although different temperature gradients should also be taken into account.

### Acknowledgements

M.S. thanks the Spanish Ministry of Education for a sabbatical stay. This work was partially funded by the Spanish DGES project 95-0028 and by the Grant Agency of the Academy of Sciences of the Czech Republic (grant A 3003903).

### References

- Collados, M., Martinez Pillet, V., Ruiz Cobo, B., del Toro Iniesta, J.C., Vazquez, M. 1994, *Astron. Astrophys.*, **291**, 622.  
Foukal, P., Little, R., Graves, J., Rabin, D., Lynch, D. 1990, *Astrophys. J.*, **353**, 712.  
Gingerich, O., Noyes, R. W., Kalkofen, W., Cuny, Y. 1971, *Solar Phys.*, **18**, 347.  
Makarova, E. A., Roshchina, E. M., Sarychev, A. P. 1994, *Solar Phys.*, **152**, 47.  
Moran, T., Foukal, P., Rabin, D. 1992, *Solar Phys.*, **142**, 1.  
Neckel, H., Labs, D. 1984, *Solar Phys.*, **90**, 205.  
Solanki, S. K., Steenbock, W. 1988, *Astron. Astrophys.*, **189**, 243.  
Wang, H., Spirock, T., Goode, P.R., Lee, C., Zirin, H., Kosonocky, W. 1998, *Astrophys. J.*, **495**, 957.